Axial gravitational quasinormal modes of a self-dual black hole in loop quantum gravity

Sen Yang,[*] Wen-Di Guo,[†] Qin Tan,[‡] and Yu-Xiao Liu[§]

Key Laboratory for Quantum Theory and Applications of the Ministry of Education, Lanzhou Center for Theoretical Physics, Lanzhou University, Lanzhou 730000, China; Key Laboratory of Theoretical Physics of Gansu Province, Institute of Theoretical Physics & Research Center of Gravitation, Lanzhou University, Lanzhou 730000, China and School of Physical Science and Technology, Lanzhou University, Lanzhou 730000, China

(Received 5 May 2023; accepted 10 July 2023; published 24 July 2023)

We study the axial gravitational quasinormal modes of a self-dual black hole in loop quantum gravity. Considering the axial perturbation of the background spacetime, we obtain the Schrödinger-like master equation. Then we calculate the quasinormal frequencies with the Wentzel-Kramers-Brillouin approximation and the asymptotic iteration method. We also investigate the numerical evolution of an initial wave packet on the self-dual black hole spacetime. We find the quantum correction parameter P positively affects the absolute values of both the real and imaginary parts of quasinormal frequencies. We derive the relation between the parameters of the circular null geodesics and quasinormal frequencies in the eikonal limit for the self-dual black hole, and numerically verify this relation.

DOI: 10.1103/PhysRevD.108.024055

I. INTRODUCTION

The first direct detection of the gravitational wave (GW) in 2015 [1] marked an all-new era of physics and astronomy [2,3]. The Event Horizon Telescope has taken the first picture of a supermassive object at the center of galaxy M87 [4–9], and the picture of the central black hole in our Milky Way [10–15]. Human beings can observe the Universe with multimessenger; both the gravitational wave and the electromagnetic wave. Until now, the LIGO-Virgo-KAGRA Collaboration has finished three observing runs and detected 90 confident GW-burst events [16–19]. GW-bursts, emitted from the merger of binary compact objects, bring information about gravitational theories and sources and provide us with a new approach to test general relativity in the strong gravitational field [20–23]. The whole gravitational wave waveform of a GW-burst event can be divided into three parts; inspiral, merger, and ringdown. The ringdown part can be successfully described by the black hole perturbation theory [24,25].

A black hole with perturbations is a dissipative system, and the eigenmodes of this system are named quasinormal modes (QNMs). The QNMs are the spectroscopy of a black hole, because the quasinormal frequencies depend only on the black hole's parameters, while their amplitudes depend on the source exciting the oscillations [26–29]. According to the behavior under space inversions, the gravitational perturbations of a spherically symmetric black hole can be divided into the odd (axial) parity part and the even (polar) parity part [24]. As the most successful theory for gravitational interaction, general relativity has passed many astrophysical tests [30]. In general relativity, Regge, Wheeler [31], and Zerilli [32] first studied the odd-parity and the even-parity gravitational perturbations of the Schwarzschild black hole. Moncrief first studied both the odd parity and the even-parity gravitational perturbations of the Reissner-Nordstrom black hole [33,34]. And Teukolsky first studied the gravitational perturbations of the Kerr black hole [35]. To get the quasinormal frequencies for the black hole perturbation problem, numerical methods are needed to solve the eigenvalue problem. With the development of the black hole perturbation theory, more and more numerical methods were proposed, such as the Wentzel-Kramers-Brillouin (WKB) approximations [36–41], the asymptotic iteration method [42], the monodromy technique [43], the series solution [44], the resonance method [45], and the Leaver's continued fraction method [46].

The singularity of general relativity is a good motivation to probe new physics. It is generally believed that a complete theory of quantum gravity has no singularity. Loop quantum gravity is exactly this case [47]. In loop quantum gravity, spacetime is made up of some basic building blocks called spin networks. In the framework of loop quantum gravity, Modesto and Premont-Schwarz constructed the Reissner-Nordstrom-like self-dual black hole [48,49]. Many works investigated the phenomenological implications of this black

[*]120220908881@lzu.edu.cn
[†]Wen-Di Guo and Sen Yang are co-first authors of this paper. guowd@lzu.edu.cn
[‡]tanq19@lzu.edu.cn
[§]Corresponding author. liuyx@lzu.edu.cn

hole [50–56]. The perturbations of the self-dual black hole also have been studied in some works, which can be divided into two categories by whether using the Arnowitt-Deser-Misner (ADM) mass of the black hole as one of the parameters fixed during calculation. Fixing the parameter $M/(1+P)^2$ instead of the ADM mass of the self-dual black hole, Chen and Wang studied the QNMs of a massless scalar field [57], Santos *et al.* studied QNMs of a massive scalar field nonminimally coupled to gravity [58], Cruz *et al.* studied axial [59] and polar gravitational perturbations [60], but it is worth pointing out that the effective potential in Ref. [59] cannot be reduced to the Schwarzschild black hole case when setting all loop quantum gravity parameters equal to zero. Fixing the ADM mass of the self-dual black hole, Liu *et al.* studied QNMs of the massless scalar field and electromagnetic field [61], and Momennia studied the QNMs of a test scalar field [62].

In this work, we focus on the axial gravitational perturbation of the self-dual black hole with fixed ADM mass, because the ADM mass is the physical mass of a black hole measured in astronomical observations. Following Ref. [48], we assume that the self-dual black hole is described by Einstein's gravity minimally coupled to an anisotropic fluid, and derive the master equation of the axial gravitational perturbation of the self-dual black hole. This method also was used to study the gravitational perturbations of nonsingular black holes in conformal gravity [63] and nonsingular Schwarzschild black holes in loop quantum gravity [64]. Then, we calculate the corresponding quasinormal frequencies with the WKB approximation and the asymptotic iteration method. The influence of the quantum correction parameter P on the QNMs is also studied. We find that the parameter P has a positive effect on the absolute values of both the real part and the imaginary part of quasinormal frequencies, which is consistent with the conclusions for the QNMs of the scalar field and the electromagnetic field on the self-dual black hole with fixed ADM mass during calculating [61,62]. Assuming the perturbation is a Gaussian packet, we investigate the numerical evolution of an initial wave packet on the self-dual black hole. Besides, Cardoso, Lemos, and Yoshida found that, in the eikonal limit, quasinormal modes of a stationary, spherically symmetric, and asymptotically flat black hole in any dimension are determined by the parameters of the circular null geodesics [65]. We obtain the relation between the quasinormal frequencies in the eikonal limit of the axial gravitational perturbation and the parameters of the circular null geodesics in the self-dual black hole, and numerically verify this relation. The numerical results show that the relation between the parameters of the circular null geodesics and quasinormal frequencies in the eikonal limit is right in the self-dual black hole in loop quantum gravity.

This paper is organized as follows. In Sec. II, we derive the master equation of the axial gravitational perturbation of the self-dual black hole. In Sec. III, we calculate the corresponding quasinormal frequencies with the WKB approximation method and the asymptotic iteration method. And we investigate the numerical evolution of an initial wave packet on the self-dual black hole spacetime. Then we obtain the relation between the parameters of the circular null geodesics and quasinormal frequencies in the eikonal limit in the self-dual black hole, and numerically verify this relation in Sec. IV. Finally, the conclusions and discussions of this work are given in Sec. V.

II. GRAVITATIONAL PERTURBATION OF LOOP QUANTUM BLACK HOLE

The line element of the spherically symmetric self-dual black hole in loop quantum gravity is [48]

$$ds^2 = -f(r)dt^2 + \frac{dr^2}{g(r)} + h(r)(d\theta^2 + \sin^2\theta d\varphi^2), \tag{2.1}$$

where the functions $f(r)$, $g(r)$, and $h(r)$ have the following forms:

$$f(r) = \frac{(r-r_+)(r-r_-)}{r^4+a_0^2}(r+r_0)^2, \tag{2.2}$$

$$g(r) = \frac{(r-r_+)(r-r_-)}{r^4+a_0^2}\frac{r^4}{(r+r_0)^2}, \tag{2.3}$$

$$h(r) = r^2 + \frac{a_0^2}{r^2}, \tag{2.4}$$

where $a_0 \simeq 5l_P^2/8\pi$ (l_p is the Planck length) is related to the minimum area gap of loop quantum gravity, $r_+ = 2M/(1+P)^2$ is the outer (event) horizon, with P a function of the polymeric parameter δ_b related to the geometric quantum effect of loop quantum gravity. $r_- = 2MP^2/(1+P)^2$ is the inner (Cauchy) horizon, $r_0 = \sqrt{r_+ r_-}$, and M is the ADM mass of the black hole. The deviation of the self-dual black hole from the Schwarzschild black hole is described by two quantum correction parameters P and a_0. The constraints on the parameter P have been obtained from various astrophysical observations [54–56], and the max one is $P < 0.0675$ [55]. Expanding Eqs. (4.16) and (2.3) in the power of $1/r$, one can see that the maximal correction from the parameter P is at the order of $(MP)/r$, while the maximal correction from a_0 is at the order of a_0^2/r^4 [55]. In this work, we focus on the physics of QNMs outside the event horizon. And the radius of the event horizon of a typical Schwarzschild black hole with the mass of the sun is of about 3 km, then $P \sim \mathcal{O}(10^{-2})$ and $a_0^2/r^4 \sim \mathcal{O}(10^{-67})$. So the effect of a_0 on astrophysical observation can be safely neglected, and we only care about the quantum correction from the parameter P.

For the self-dual black hole, one can simulate the quantum corrections with an effective anisotropic matter fluid, and write the field equation as the Einstein equation form $G_{\mu\nu} = 8\pi T_{\mu\nu}$, where $T_{\mu\nu}$ is the effective energy-momentum tensor [48]. Because of symmetries of the background spacetime, the effective energy-momentum tensor of this anisotropic perfect fluid can be written as

$$T_{\mu\nu} = (\rho + p_2)u_\mu u_\nu + (p_1 - p_2)x_\mu x_\nu + p_2\hat{g}_{\mu\nu}, \quad (2.5)$$

where ρ is the energy density measured by a comoving observer with the fluid, p_1 and p_2 are the radial pressure and the tangential pressure, respectively. u_μ is the timelike four-velocity and x_μ is the spacelike unit vector orthogonal to u_μ and angular directions. And $\hat{g}_{\mu\nu}$ is the metric of the background spacetime. The timelike four-velocity u_μ and the spacelike unit vector x_μ satisfy

$$u_\mu u^\mu = -1 \quad \text{and} \quad x_\mu x^\mu = 1. \quad (2.6)$$

We can assume $u^\mu = (u^t, 0, 0, 0)$ and $x^\mu = (0, x^r, 0, 0)$ in the comoving frame. To study the perturbations of a spherically symmetric black hole, one can first focus on axisymmetric modes of perturbations [24]. We consider a perturbed spacetime which is described by a nonstationary and axisymmetric metric as

$$ds^2 = -e^{2\nu}(dx^0)^2 + e^{2\psi}(d\varphi - \sigma dx^0 - q_2 dx^2 - q_3 dx^3)^2 + e^{2\mu_2}(dx^2)^2 + e^{2\mu_3}(dx^3)^2, \quad (2.7)$$

where ν, ψ, μ_2, μ_3, σ, q_2, and q_3 depend on time coordinate t $(t = x^0)$, radial coordinate r $(r = x^2)$, and polar angle coordinate $\theta(\theta = x^3)$. And a tetrad basis $e^\mu_{(a)}$ corresponding to the metric (2.7) is

$$\begin{aligned} e^\mu_{(0)} &= (e^{-\nu}, \sigma e^{-\nu}, 0, 0), \\ e^\mu_{(1)} &= (0, e^{-\psi}, 0, 0), \\ e^\mu_{(2)} &= (0, q_2 e^{-\mu_2}, e^{-\mu_2}, 0), \\ e^\mu_{(3)} &= (0, q_3 e^{-\mu_3}, 0, e^{-\mu_3}). \end{aligned} \quad (2.8)$$

In this regard, one can project any vector or tensor field onto the tetrad frame by

$$A_{(a)} = e^\mu_{(a)} A_\mu, \qquad B_{(a)(b)} = e^\mu_{(a)} e^\nu_{(b)} B_{\mu\nu}. \quad (2.9)$$

For a static and spherically symmetric spacetime, σ, q_2, and q_3 are zero. Then, comparing the metric (2.7) with (2.1), one can get

$$e^{2\nu} = f(r), \qquad e^{-2\mu_2} = g(r), \qquad e^{2\mu_3} = h(r), \qquad e^{2\psi} = h(r)\sin^2\theta. \quad (2.10)$$

Generally, the gravitational perturbations will affect symmetries of the background spacetime and form of the modified Einstein equation. Because there is no well-defined field equation in loop quantum gravity, we assume the quantum corrections to Einstein equation are also the anisotropic fluid form in the perturbation level. The perturbed energy-momentum tensor of the anisotropic fluid in the tetrad frame is

$$\delta T_{(a)(b)} = (\rho + p_2)\delta(u_{(a)}u_{(b)}) + (\delta\rho + \delta p_2)u_{(a)}u_{(b)} + (p_1 - p_2)\delta(x_{(a)}x_{(b)}) + (\delta p_1 - \delta p_2)x_{(a)}x_{(b)} + \delta p_2 \eta_{(a)(b)}. \quad (2.11)$$

With Eq. (2.6) and $u^\mu x_\mu = 0$, one can find that the axial components of Eq. (2.11) vanish

$$\delta T_{(1)(0)} = \delta T_{(1)(2)} = \delta T_{(1)(3)} = 0. \quad (2.12)$$

In the tetrad frame, the modified Einstein equation is written as

$$R_{(a)(b)} - \frac{1}{2}\eta_{(a)(b)}R = 8\pi T_{(a)(b)}. \quad (2.13)$$

With Eq. (2.12), we can obtain the master equation of the axial gravitational perturbation of the self-dual black hole from the axial components of $R_{(a)(b)} = 0$. Note that the axial components of $R_{(a)(b)}$ here include perturbations of σ, q_2, and q_3. The (1,3) and (1,2) components of $R_{(a)(b)}|_{\text{axial}} = 0$ are

$$[he^{\nu-\mu_2}(q_{2,3} - q_{3,2})]_{,2} = [he^{\mu_2-\nu}(\sigma_{,3} - q_{3,0})]_{,0}, \quad (2.14)$$

$$[he^{\nu-\mu_2}(q_{3,2} - q_{2,3})\sin^3\theta]_{,3} = [h^2 e^{-\nu-\mu_2}(\sigma_{,2} - q_{2,0})\sin^3\theta]_{,0}, \quad (2.15)$$

respectively, where $F_{,i} \equiv \frac{\partial F}{\partial x^i}$. Then, one can define

$$Q = he^{\nu-\mu_2}(q_{2,3} - q_{3,2})\sin^3\theta, \quad (2.16)$$

and rewrite Eqs. (2.14) and (2.15) as

$$e^{\nu-\mu_2}\frac{Q_{,2}}{h\sin^3\theta} = (\sigma_{,3} - q_{3,0})_{,0}, \quad (2.17)$$

$$e^{\nu+\mu_2}\frac{Q_{,3}}{h^2\sin^3\theta} = -(\sigma_{,2} - q_{2,0})_{,0}. \quad (2.18)$$

By differentiating Eqs. (2.17) and (2.18) and eliminating σ, one can obtain

$$\frac{1}{\sin^3\theta}\left(\frac{e^{\nu-\mu_2}}{h}Q_{,2}\right)_{,2}+\frac{e^{\nu+\mu_2}}{h^2}\left(\frac{Q_{,3}}{\sin^3\theta}\right)_{,3}=\frac{Q_{,00}}{he^{\nu-\mu_2}\sin^3\theta}. \tag{2.19}$$

Considering the ansatz [24]

$$Q(r,\theta)=Q(r)Y(\theta) \tag{2.20}$$

with $Y(\theta)$ the Gegenbauer function satisfying

$$\frac{d}{d\theta}\left(\frac{1}{\sin^3\theta}\frac{dY}{d\theta}\right)=-\mu^2\frac{Y}{\sin^3\theta}, \tag{2.21}$$

where $\mu^2=(l-1)(l+2)$, one can rewrite Eq. (2.19) as

$$\left(\frac{e^{\nu-\mu_2}}{h}Q_{,r}\right)_{,r}+\left(\frac{\omega^2}{he^{\nu-\mu_2}}-\frac{e^{\nu+\mu_2}\mu^2}{h^2}\right)Q=0. \tag{2.22}$$

Note that here we have used the Fourier transformation $\partial t\to -i\omega$. Then, one can define

$$\Psi(r)=\frac{Q(r)}{\sqrt{h(r)}}. \tag{2.23}$$

With this, we can obtain the Schrödinger-like master equation of the axial gravitational perturbation for the self-dual black hole

$$\frac{\partial^2\Psi}{\partial r_*^2}+[\omega^2-V(r)]\Psi=0, \tag{2.24}$$

where

$$V(r)=\frac{f(r)(l-1)(l+2)}{h(r)}-\sqrt{f(r)g(r)h(r)}\frac{d}{dr}\times\left(\frac{\sqrt{f(r)g(r)}}{h(r)}\frac{d\sqrt{h(r)}}{dr}\right) \tag{2.25}$$

is the effective potential, and r_* is the tortoise coordinate defined by

$$\begin{aligned}r_*&=\int\frac{dr}{\sqrt{f(r)g(r)}}\\&=r-\frac{a_0^2}{r_+r_-}\left(\frac{1}{r}-\frac{r_++r_-}{r_+r_-}\ln(r)\right)\\&\quad+\frac{1}{(r_+-r_-)}\left(\frac{a_0^2+r_+^4}{r_+^2}\ln(r-r_+)\right.\\&\quad\left.-\frac{a_0^2+r_-^4}{r_-^2}\ln(r-r_-)\right).\end{aligned} \tag{2.26}$$

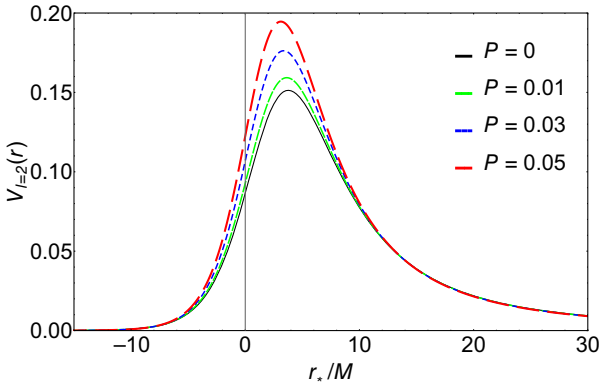

FIG. 1. The effective potential (4.15) in the tortoise coordinate (2.26) with $M=1$, $l=2$, and different values of the parameter P. The black curve shows the Regge-Wheeler potential of the Schwarzschild black hole.

It is worthwhile to mention that r_* running from $-\infty$ to $+\infty$ matches r from the event horizon to spatial infinity. With different values of the parameter P, the plots for the effective potential (4.15) in the tortoise coordinate (2.26) are shown in Fig. 1. It can be seen that, the height of the effective potential increases with the parameter P.

III. QUASINORMAL MODES AND RINGDOWN WAVEFORMS

A. Quasinormal modes

The Schrödinger-like equation (2.24) has a set of complex eigenvalues, which are the QNMs of the self-dual black holes (2.1). In this work, we calculate the QNMs of the self-dual black hole using the WKB approximation method and the asymptotic iteration method.

The WKB approximation method was first applied to the problem of scattering around a black hole at the first order by Schutz and Will [37], and later developed to higher orders [38–41]. This method can be used to solve the eigenvalue problem in which the effective potential has the form of a potential barrier and approaches to constant values at the event horizon and spatial infinity. The effective potential (4.15) satisfies these conditions. And the WKB approximation works best for low overtones, i.e., modes with a long decay time, and in the eikonal limit of large l. Setting $a_0=0$, P from 0 to 0.05, and $\{l=2,3,4\}(0\le n<l)$, we use the WKB approximation to calculate the quasinormal frequencies ω_{nl} for the axial gravitational perturbation of the self-dual black hole. The results are listed in Tables I–III.

To use the asymptotic iteration method, we first rewrite the Schrödinger-like equation (2.24) in the r coordinate as follows:

$$f(r)g(r)\Psi''(r)+\frac{1}{2}[f'(r)g(r)+f(r)g'(r)]\Psi'(r)+[\omega^2-V(r)]\Psi=0, \tag{3.1}$$

TABLE I. The QNMs of the axial gravitational perturbation of the self-dual black hole with different values of P and $l = 2$ $(n < l)$ calculated by the WKB approximation method and the asymptotic iteration method.

P		0	0.001	0.002	0.003	0.004
ω_{02}	WKB	$0.747239 - 0.177782i$	$0.749070 - 0.178631i$	$0.751042 - 0.179012i$	$0.753013 - 0.179395i$	$0.754989 - 0.179778i$
	AIM	$0.747343 - 0.177925i$	$0.749308 - 0.178310i$	$0.751275 - 0.178696i$	$0.753245 - 0.179083i$	$0.755219 - 0.179469i$
ω_{12}	WKB	$0.692593 - 0.546960i$	$0.694458 - 0.550582i$	$0.696397 - 0.551722i$	$0.698308 - 0.552887i$	$0.700231 - 0.554047i$
	AIM	$0.693422 - 0.547830i$	$0.695331 - 0.549007i$	$0.697244 - 0.550185i$	$0.699160 - 0.551364i$	$0.701079 - 0.552544i$
P		0.005	0.006	0.007	0.008	0.009
ω_{02}	WKB	$0.756968 - 0.180161i$	$0.758947 - 0.180545i$	$0.760937 - 0.180927i$	$0.762917 - 0.181313i$	$0.764911 - 0.181696i$
	AIM	$0.757195 - 0.179856i$	$0.759175 - 0.180243i$	$0.761158 - 0.180630i$	$0.763144 - 0.181018i$	$0.765133 - 0.181406i$
ω_{12}	WKB	$0.702162 - 0.555202i$	$0.704074 - 0.556377i$	$0.706039 - 0.557514i$	$0.707924 - 0.558717i$	$0.709883 - 0.559865i$
	AIM	$0.703001 - 0.553724i$	$0.704927 - 0.554905i$	$0.706856 - 0.556086i$	$0.708788 - 0.557269i$	$0.710723 - 0.558451i$
P		0.01	0.02	0.03	0.04	0.05
ω_{02}	WKB	$0.766907 - 0.182080i$	$0.787023 - 0.185939i$	$0.807444 - 0.189824i$	$0.828184 - 0.193732i$	$0.849226 - 0.197664i$
	AIM	$0.767126 - 0.181794i$	$0.787220 - 0.185688i$	$0.807626 - 0.189606i$	$0.828342 - 0.193545i$	$0.849370 - 0.197505i$
ω_{12}	WKB	$0.711840 - 0.561018i$	$0.731465 - 0.572694i$	$0.751382 - 0.584477i$	$0.771677 - 0.596294i$	$0.792250 - 0.608217i$
	AIM	$0.712662 - 0.559635i$	$0.732229 - 0.571507i$	$0.752124 - 0.583441i$	$0.772348 - 0.595432i$	$0.792902 - 0.607476i$

TABLE II. The QNMs of the axial gravitational perturbation of the self-dual black hole with different values of P and $l = 3$ $(n < l)$ calculated by the WKB approximation method and the asymptotic iteration method.

P		0	0.001	0.002	0.003	0.004
ω_{03}	WKB	$1.198890 - 0.185405i$	$1.202070 - 0.185814i$	$1.205260 - 0.186225i$	$1.208450 - 0.186637i$	$1.211660 - 0.187049i$
	AIM	$1.198890 - 0.185406i$	$1.202070 - 0.185818i$	$1.205260 - 0.186229i$	$1.208460 - 0.186641i$	$1.211660 - 0.187054i$
ω_{13}	WKB	$1.165280 - 0.562581i$	$1.168370 - 0.563804i$	$1.171530 - 0.565043i$	$1.174660 - 0.566297i$	$1.177840 - 0.567532i$
	AIM	$1.165290 - 0.562596i$	$1.168430 - 0.563839i$	$1.171580 - 0.565083i$	$1.174740 - 0.566327i$	$1.177900 - 0.567572i$
ω_{23}	WKB	$1.103190 - 0.958094i$	$1.105190 - 0.959163i$	$1.108290 - 0.961239i$	$1.111290 - 0.963398i$	$1.114440 - 0.965438i$
	AIM	$1.103370 - 0.958185i$	$1.106440 - 0.960284i$	$1.109520 - 0.962384i$	$1.112600 - 0.964485i$	$1.115690 - 0.966587i$
P		0.005	0.006	0.007	0.008	0.009
ω_{03}	WKB	$1.214860 - 0.187462i$	$1.218080 - 0.187874i$	$1.221290 - 0.188287i$	$1.224510 - 0.188700i$	$1.227740 - 0.189113i$
	AIM	$1.214870 - 0.187466i$	$1.218080 - 0.187879i$	$1.221300 - 0.188292i$	$1.224520 - 0.188705i$	$1.227740 - 0.189119i$
ω_{13}	WKB	$1.180990 - 0.568787i$	$1.184200 - 0.570014i$	$1.187340 - 0.571279i$	$1.190530 - 0.572520i$	$1.193730 - 0.573760i$
	AIM	$1.181060 - 0.568818i$	$1.184230 - 0.570065i$	$1.187410 - 0.571312i$	$1.190590 - 0.572560i$	$1.193780 - 0.573809i$
ω_{23}	WKB	$1.117460 - 0.967595i$	$1.120690 - 0.969581i$	$1.123660 - 0.971795i$	$1.126810 - 0.973858i$	$1.129980 - 0.975910i$
	AIM	$1.118780 - 0.968691i$	$1.121880 - 0.970795i$	$1.124980 - 0.972901i$	$1.128090 - 0.975008i$	$1.131200 - 0.977116i$
P		0.01	0.02	0.03	0.04	0.05
ω_{03}	WKB	$1.230970 - 0.189527i$	$1.263560 - 0.193675i$	$1.296650 - 0.197847i$	$1.330240 - 0.202038i$	$1.364330 - 0.206247i$
	AIM	$1.230970 - 0.189533i$	$1.263560 - 0.193683i$	$1.296660 - 0.197856i$	$1.330250 - 0.202049i$	$1.364340 - 0.206260i$
ω_{13}	WKB	$1.196890 - 0.575022i$	$1.229120 - 0.587533i$	$1.261790 - 0.600136i$	$1.295010 - 0.612780i$	$1.328740 - 0.625475i$
	AIM	$1.196970 - 0.575058i$	$1.229160 - 0.587590i$	$1.261860 - 0.600186i$	$1.295080 - 0.612838i$	$1.328790 - 0.625548i$
ω_{23}	WKB	$1.133000 - 0.978100i$	$1.164550 - 0.999115i$	$1.196440 - 1.020400i$	$1.228970 - 1.041680i$	$1.262040 - 1.063030i$
	AIM	$1.134320 - 0.979225i$	$1.165780 - 1.000370i$	$1.197770 - 1.021610i$	$1.230290 - 1.042940i$	$1.263430 - 1.064120i$

where the prime denotes the derivative to r. For the perturbation propagating in the black hole spacetime, there are two physical boundary conditions: (i) $\Psi(r_*) \sim e^{-i\omega r_*}$ as $r_* \to -\infty (r \to r_+)$, which means the wave near the event horizon should purely enter the black hole; (ii) $\Psi(r_*) \sim e^{i\omega r_*}$ as $r_* \to \infty (r \to \infty)$, which means the wave is purely outgoing at spatial infinity. For $a_0 = 0$ and $P \neq 0$, the self-dual black hole has both a Cauchy horizon and an event horizon, and one can define the solution of Eq. (3.1) as

$$\Psi(r) = \frac{e^{i\omega r}}{r}(r - r_-)^{1+i\omega+i\omega r_+^2/(r_+-r_-)} \times (r - r_+)^{-i\omega r_+^2/(r_+-r_-)}\psi(r). \tag{3.2}$$

TABLE III. The QNMs of the axial gravitational perturbation of the self-dual black hole with different values of P and $l = 4$ $(n < l)$ calculated by the WKB approximation method and the asymptotic iteration method.

P		0	0.001	0.002	0.003	0.004
ω_{04}	WKB	$1.618360 - 0.188328i$	$1.622670 - 0.188743i$	$1.626980 - 0.189162i$	$1.631310 - 0.189581i$	$1.635640 - 0.190001i$
	AIM	$1.618360 - 0.188328i$	$1.622670 - 0.188747i$	$1.626990 - 0.189166i$	$1.631310 - 0.189586i$	$1.635640 - 0.190006i$
ω_{14}	WKB	$1.593260 - 0.568668i$	$1.597520 - 0.569909i$	$1.601810 - 0.571169i$	$1.606090 - 0.572435i$	$1.610410 - 0.573693i$
	AIM	$1.593260 - 0.568669i$	$1.597540 - 0.569930i$	$1.601830 - 0.571193i$	$1.606120 - 0.572456i$	$1.610420 - 0.573720i$
ω_{24}	WKB	$1.545390 - 0.959799i$	$1.549230 - 0.961465i$	$1.553480 - 0.963572i$	$1.557680 - 0.965712i$	$1.561980 - 0.967793i$
	AIM	$1.545420 - 0.959816i$	$1.549640 - 0.961934i$	$1.553870 - 0.964053i$	$1.558100 - 0.966173i$	$1.562340 - 0.968294i$
ω_{34}	WKB	$1.479330 - 1.367800i$	$1.480970 - 1.368580i$	$1.485160 - 1.371530i$	$1.489220 - 1.374600i$	$1.493530 - 1.377460i$
	AIM	$1.479670 - 1.367850i$	$1.483820 - 1.370840i$	$1.487970 - 1.373830i$	$1.492120 - 1.376830i$	$1.496290 - 1.379820i$
P		0.005	0.006	0.007	0.008	0.009
ω_{04}	WKB	$1.639980 - 0.190421i$	$1.644320 - 0.190841i$	$1.648680 - 0.191261i$	$1.653040 - 0.191682i$	$1.657400 - 0.192103i$
	AIM	$1.639980 - 0.190426i$	$1.644320 - 0.190846i$	$1.648680 - 0.191266i$	$1.653030 - 0.191687i$	$1.657400 - 0.192108i$
ω_{14}	WKB	$1.614720 - 0.574957i$	$1.619010 - 0.5762290i$	$1.623350 - 0.577488i$	$1.627680 - 0.578753i$	$1.632010 - 0.580023i$
	AIM	$1.614730 - 0.574985i$	$1.619040 - 0.576250i$	$1.623360 - 0.577516i$	$1.627690 - 0.578783i$	$1.632030 - 0.580050i$
ω_{24}	WKB	$1.566230 - 0.969911i$	$1.570410 - 0.972080i$	$1.574750 - 0.974154i$	$1.579030 - 0.976273i$	$1.583280 - 0.978414i$
	AIM	$1.566590 - 0.970416i$	$1.570840 - 0.972540i$	$1.575110 - 0.974664i$	$1.579380 - 0.976790i$	$1.583650 - 0.978917i$
ω_{34}	WKB	$1.497710 - 1.380440i$	$1.501700 - 1.383610i$	$1.506070 - 1.386430i$	$1.510280 - 1.389400i$	$1.514410 - 1.392460i$
	AIM	$1.500460 - 1.382820i$	$1.504640 - 1.385820i$	$1.508820 - 1.388820i$	$1.513200 - 1.391820i$	$1.517220 - 1.394830i$
P		0.01	0.02	0.03	0.04	0.05
ω_{04}	WKB	$1.661770 - 0.192524i$	$1.705860 - 0.196748i$	$1.750630 - 0.200992i$	$1.796060 - 0.205255i$	$1.842160 - 0.209535i$
	AIM	$1.661770 - 0.192529i$	$1.705860 - 0.196753i$	$1.750630 - 0.200998i$	$1.796060 - 0.205262i$	$1.842160 - 0.209537i$
ω_{14}	WKB	$1.636360 - 0.581289i$	$1.680140 - 0.594005i$	$1.724610 - 0.606781i$	$1.769770 - 0.619610i$	$1.815590 - 0.632491i$
	AIM	$1.636370 - 0.581318i$	$1.680150 - 0.594035i$	$1.724630 - 0.606813i$	$1.769780 - 0.619645i$	$1.815590 - 0.632407i$
ω_{24}	WKB	$1.587580 - 0.980530i$	$1.630780 - 1.001860i$	$1.674690 - 1.023290i$	$1.719310 - 1.044790i$	$1.764590 - 1.066390i$
	AIM	$1.587940 - 0.981045i$	$1.631150 - 1.002380i$	$1.675070 - 1.023810i$	$1.719690 - 1.045310i$	$1.765060 - 1.065550i$
ω_{34}	WKB	$1.518650 - 1.395430i$	$1.561030 - 1.425560i$	$1.604130 - 1.455810i$	$1.648010 - 1.486120i$	$1.692500 - 1.516630i$
	AIM	$1.521430 - 1.397830i$	$1.563900 - 1.427990i$	$1.607090 - 1.458230i$	$1.651150 - 1.488830i$	$1.699090 - 1.510890i$

Taking the solution (3.2), we use the asymptotic iteration method to solve Eq. (3.1) and obtain the corresponding quasinormal frequencies with the same setting in the previous WKB calculation. The results are also listed in Tables I–III.

In Tables I–III, one can find that when $P = 0$, the quasinormal frequencies we obtained agree well with the quasinormal frequencies for the axial gravitational perturbation of the Schwarzschild black hole [39,66]. This is in line with expectations because the metric (2.1) goes back to the Schwarzschild black hole when both the two quantum parameters vanish. For $l = 2, 3, 4$ and $n = 0$, the absolute values of both the real part and the imaginary part of the quasinormal frequencies varying with the value of P are shown in Fig. 2. It can be seen that the absolute values of both the real and imaginary parts of the quasinormal frequencies increase with the parameter P. This means the parameter P has a positive effect on the absolute values of both the real and imaginary parts of quasinormal frequencies of the axial gravitational perturbation of the self-dual black hole. This is consistent with the conclusions for the QNMs of the perturbations of the test scalar field and the electromagnetic field of the self-dual black hole [61,62] by taking the ADM mass M of the self-dual black hole as a fixed parameter in numerical analysis. But it is different from the results in works [57–60] in which $M/(1+P)^2$ was taken as a fixed parameter. The shapes of the plots in Fig. 2 depend on whether we vary the value of P at fixed M, or at fixed $M/(1+P)^2$. On the other hand, although the effective potential (4.15) is different from the one in [59], both the effective potential (4.15) and the one in [59] should be consistent with the Regge–Wheeler potential of the Schwarzschild black hole in $a_0 \to 0$ and $P \to 0$ limit. But it is worth mentioning that the effective potential in [59] can not go back to the Schwarzschild case when both the two quantum parameters vanish, and the effective potential (4.15) can do this. Our work and Ref. [59] have used the same field equation $G_{\mu\nu} = T_{\mu\nu}$. Because both the works end up setting the axial components of the Ricci tensor to zero, the difference between the two is a result of the particular choice of basis and keeping M or $M/(1+P)^2$ as a constant in numerical analysis.

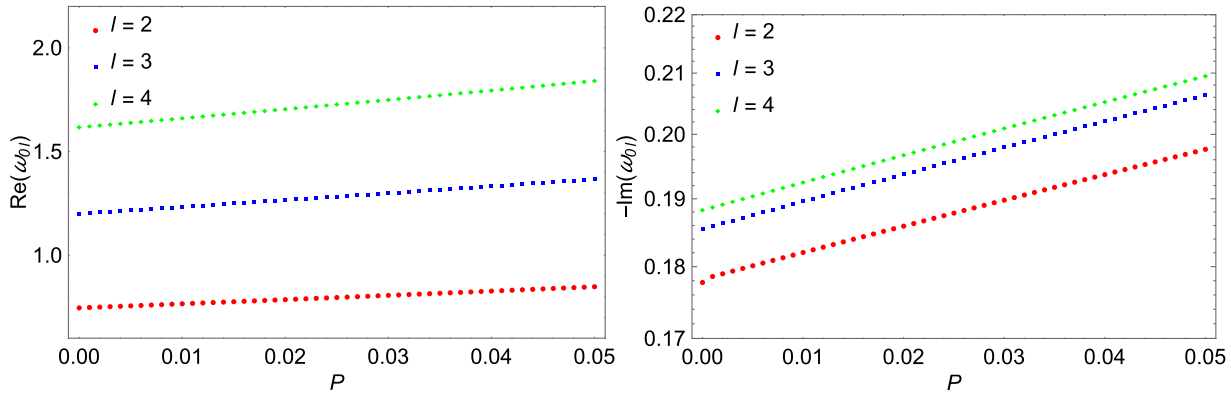

FIG. 2. The left plot shows the real parts of ω_{02}, ω_{03}, ω_{04} in with the parameter P. The right plot shows the absolute values of the imaginary parts of ω_{02}, ω_{03}, ω_{04} in with the parameter P.

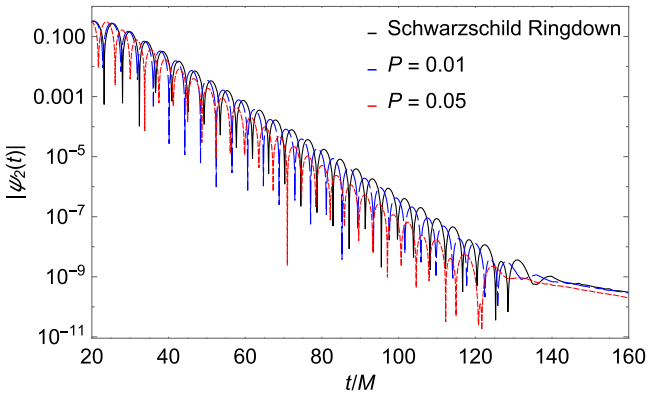

FIG. 3. The time evolution of the wave function $\Psi_2(t)$ ($l = 2$) of the axial gravitational perturbation for the self-dual black hole with different values of the parameter P, evaluated at $r = 10r_+$. The black curve ($P = 0$) shows the Schwarzschild ringdown case.

B. Ringdown waveforms

To investigate the contribution of all modes of the axial perturbation of the self-dual black hole, we can consider the numeric evolution of an initial wave packet in the self-dual black hole spacetime. In a finite time domain, the Schrödinger-like equation (2.24) can be rewritten as

$$\frac{\partial^2\Psi}{\partial r_*^2} - \frac{\partial^2\Psi}{\partial t^2} - V(r_*)\Psi = 0. \tag{3.3}$$

Using the light-cone coordinates $u = t - r_*$ and $v = t + r_*$ [67], the above equation can be written as

$$4\frac{\partial^2\Psi(u,v)}{\partial u\partial v} - V(u,v)\Psi(u,v) = 0. \tag{3.4}$$

Here, we set the initial data for Eq. (3.4) as

$$\Psi(u,0) = 0 \quad \text{and} \quad \Psi(0,v) = \exp\left(-\frac{(v-v_c)^2}{2\beta^2}\right), \tag{3.5}$$

where $\Psi(0,v)$ is a Gaussian wave packet centered in v_c and having width β. Then, we choose the observer located at $r = 10r_+$ and numerically solve the partial differential equation (3.4) to generate the ringdown waveforms. As shown in Fig. 3, the waveform with a larger value of the parameter P damps more quickly. Finally, without loss of generality, we use a modified exponentially decaying function $e^{\omega_I t}A\sin(\omega_R + B)$ to fit the data in Fig. 3 and calculate the fundamental mode ω_{02} with different values of the parameter P, which plays a major role in the ringdown waveforms. The results are shown in Table IV. Considering the error in the numerical calculation process, one can find that the fitting values of the fundamental mode ω_{02} with different values of the parameter P in Table IV agree well with the results obtained by using the WKB approximation method and the asymptotic iteration method.

TABLE IV. The fundamental mode ω_{02} calculated by fitting the data in Fig. 3, WKB approximation method, and the asymptotic iteration method.

P		0	0.01	0.05
ω_{02}	Fitting	$0.747304 - 0.178066i$	$0.765487 - 0.182486i$	$0.844821 - 0.199696i$
	WKB	$0.747239 - 0.177782i$	$0.766907 - 0.182080i$	$0.849226 - 0.197664i$
	AIM	$0.747343 - 0.177925i$	$0.767126 - 0.181794i$	$0.849370 - 0.197505i$

IV. QNMs IN THE EIKONAL LIMIT AND CIRCULAR NULL GEODESICS

Assuming a stationary, spherically symmetric, and asymptotically flat line element, Cardoso *et al.* showed that, in the eikonal limit $l \to \infty$, the QNMs of a black hole in any dimensions are [65]

$$\omega_{\mathrm{QNM}} = \Omega_c l - i(n+1/2)|\lambda_c|, \tag{4.1}$$

where the subscript c means that the quantity is evaluated at the radius $r = r_c$ of a circular null geodesic, Ω_c and λ_c are the coordinate angular velocity and the Lyapunov exponent of the circular null geodesics, respectively. It is an interesting relation between quasinormal frequencies and the parameters of the circular null geodesics, but it may be not valid in a specific black hole [68]. In this section, based on Eq. (4.1), we shall derive the explicit relation between the QNMs, in the eikonal limit, and the parameters of the circular null geodesics of the self-dual black hole. Then we numerically verify this relation.

The Lagrangian for a photon in the equatorial plane ($\theta = \pi/2$) in the self-dual black hole is

$$\mathcal{L} = \frac{1}{2}\left[-f(r)\dot{t}^2 + \frac{1}{g(r)}\dot{r}^2 + h(r)\dot{\varphi}^2\right], \tag{4.2}$$

and the generalized momentum from this Lagrangian is

$$p_t = -f(r)\dot{t} = -E, \tag{4.3}$$

$$p_\varphi = h(r)\dot{\varphi} = L, \tag{4.4}$$

$$p_r = \frac{\dot{r}}{g(r)}, \tag{4.5}$$

where E is the energy, L is the angular momentum, and the dot denotes differentiation to an affine parameter along the geodesics of the photon. Because the Lagrangian (4.2) is independent of both t and φ, E and L are conserved. From Eqs. (4.3) and (4.4), one can get

$$\dot{\varphi} = \frac{L}{h(r)}, \qquad \dot{t} = \frac{E}{f(r)}. \tag{4.6}$$

The Hamiltonian for the photon is

$$\mathcal{H} = \frac{1}{2}\left[-E\dot{t} + L\dot{\varphi} + \frac{1}{g(r)}\dot{r}^2\right] = 0. \tag{4.7}$$

With Eqs. (4.6) and (4.7), one can define the effective potential as

$$V_r \equiv \dot{r}^2 = g(r)\left[\frac{E^2}{f(r)} - \frac{L^2}{h(r)}\right]. \tag{4.8}$$

For the circular ($r = r_c$) null geodesics on the equatorial plane, the conditions $V_r = V_r' = 0$ lead to

$$\frac{E}{L} = \pm\sqrt{\frac{f_c}{h_c}}, \qquad f_c h_c' = f_c' h_c. \tag{4.9}$$

In this case

$$V_r'' = \frac{L^2 g_c}{f_c h_c^2}(f_c h_c'' - f_c'' h_c), \tag{4.10}$$

and the coordinate angular velocity is

$$\Omega_c = \frac{\dot{\varphi}}{\dot{t}} = \left(\frac{f_c}{h_c}\right)^{1/2}. \tag{4.11}$$

The principal Lyapunov exponent is a quantity that characterizes the rate of separation of infinitesimally close geodesics. Using the expression of the principal Lyapunov exponent [65]

$$\lambda = \sqrt{\frac{V_r''}{2\dot{t}^2}}, \tag{4.12}$$

we get

$$\lambda_c = \sqrt{\frac{g_c}{2h_c}(f_c h_c'' - f_c'' h_c)} \tag{4.13}$$

for the circular null geodesics of the self-dual black hole. Taking Eqs. (4.11) and (4.13) into (4.1), we derive the relation between the QNMs, in the eikonal limit, and the parameters of the circular null geodesics of the self-dual black hole

$$\omega_{\mathrm{QNM}} = l\left(\frac{f_c}{h_c}\right)^{1/2} - i(n+1/2)\sqrt{\frac{g_c}{2h_c}(f_c h_c'' - f_c'' h_c)}. \tag{4.14}$$

Setting $l = 100$ and $n = 0, 1, 2, 3, 4$, we calculate the quasinormal frequencies in the eiknoal limit by the WKB approximation method and the relation (4.14). We list the numerical results in Tables V and VI. Considering the error of calculation, one can find that the quasinormal frequencies obtained by the WKB approximation method and the relation (4.14) agree well with each other in Tables V and VI. It means that the general relation (4.1), between quasinormal frequencies and the parameters of the circular null geodesics, is right for the self-dual black hole in loop quantum gravity.

Actually, in the eikonal limit $l \to \infty$, the effective potentials of scalar, electromagnetic and gravitational perturbations of a stationary, spherically symmetric, and asymptotically flat black hole have the same behavior [65]

TABLE V. The QNMs ω_{nl} of the axial gravitational perturbation of the self-dual black hole with different values of the parameter P and $l = 100$, calculated by the WKB approximation method and the QNMs-circular null geodesics (CNG) relation (4.14).

P		0	0.001	0.002	0.003	0.004
$\omega_{0,100}$	WKB	$38.6775 - 0.19244i$	$38.7807 - 0.19287i$	$38.8841 - 0.19330i$	$38.9876 - 0.19373i$	$39.0913 - 0.19416i$
	CNG	$38.4900 - 0.19245i$	$38.5927 - 0.19288i$	$38.6956 - 0.19331i$	$38.7987 - 0.19373i$	$38.9019 - 0.19416i$
$\omega_{1,100}$	WKB	$38.6764 - 0.57733i$	$38.7796 - 0.57862i$	$38.8830 - 0.57990i$	$38.9866 - 0.58119i$	$39.0903 - 0.58247i$
	CNG	$38.4900 - 0.57735i$	$38.5927 - 0.57863i$	$38.6956 - 0.57992i$	$38.7987 - 0.58120i$	$38.9019 - 0.58249i$
$\omega_{2,100}$	WKB	$38.6743 - 0.96225i$	$38.7775 - 0.96439i$	$38.8809 - 0.96653i$	$38.9844 - 0.96867i$	$39.0881 - 0.97081i$
	CNG	$38.4900 - 0.96225i$	$38.5927 - 0.96439i$	$38.6956 - 0.96653i$	$38.7987 - 0.96867i$	$38.9019 - 0.97081i$
$\omega_{3,100}$	WKB	$38.6711 - 1.34719i$	$38.7743 - 1.35019i$	$38.8777 - 1.35318i$	$38.9812 - 1.35618i$	$39.0849 - 1.35918i$
	CNG	$38.4900 - 1.34715i$	$38.5927 - 1.35015i$	$38.6956 - 1.35314i$	$38.7987 - 1.35614i$	$38.9019 - 1.35914i$
$\omega_{4,100}$	WKB	$38.6668 - 1.73219i$	$38.7701 - 1.73603i$	$38.8734 - 1.73989i$	$38.9770 - 1.74374i$	$39.0806 - 1.74760i$
	CNG	$38.4900 - 1.73205i$	$38.5927 - 1.73590i$	$38.6956 - 1.73975i$	$38.7987 - 1.74361i$	$38.9019 - 1.74746i$
P		0.005	0.006	0.007	0.008	0.009
$\omega_{0,100}$	WKB	$39.1952 - 0.19458i$	$39.2992 - 0.19501i$	$39.4034 - 0.19544i$	$39.5077 - 0.19587i$	$39.6122 - 0.19630i$
	CNG	$39.0052 - 0.19459i$	$39.1087 - 0.19502i$	$39.2124 - 0.19545i$	$39.3162 - 0.19588i$	$39.4202 - 0.19631i$
$\omega_{1,100}$	WKB	$39.1941 - 0.58376i$	$39.2981 - 0.58504i$	$39.4023 - 0.58633i$	$39.5067 - 0.58762i$	$39.6112 - 0.58891i$
	CNG	$39.0052 - 0.58377i$	$39.1087 - 0.58506i$	$39.2124 - 0.58635i$	$39.3162 - 0.58764i$	$39.4202 - 0.58892i$
$\omega_{2,100}$	WKB	$39.1920 - 0.97295i$	$39.2960 - 0.97510i$	$39.4002 - 0.97724i$	$39.5045 - 0.97939i$	$39.6090 - 0.98154i$
	CNG	$39.0052 - 0.97296i$	$39.1087 - 0.97510i$	$39.2124 - 0.97725i$	$39.3162 - 0.97939i$	$39.4202 - 0.98154i$
$\omega_{3,100}$	WKB	$39.1888 - 1.36218i$	$39.2928 - 1.36518i$	$39.3970 - 1.36819i$	$39.5013 - 1.37119i$	$39.6058 - 1.37420i$
	CNG	$39.0052 - 1.36214i$	$39.1087 - 1.36514i$	$39.2124 - 1.36814i$	$39.3162 - 1.37115i$	$39.4202 - 1.37416i$
$\omega_{4,100}$	WKB	$39.1845 - 1.75146i$	$39.2885 - 1.75532i$	$39.3927 - 1.75918i$	$39.4970 - 1.76305i$	$39.6015 - 1.76691i$
	CNG	$39.0052 - 1.75132i$	$39.1087 - 1.75518i$	$39.2124 - 1.75904i$	$39.3162 - 1.76291i$	$39.4202 - 1.76677i$
P		0.01	0.02	0.03	0.04	0.05
$\omega_{0,100}$	WKB	$39.7169 - 0.19673i$	$40.7723 - 0.20104i$	$41.8436 - 0.20537i$	$42.9308 - 0.20971i$	$44.0338 - 0.21406i$
	CNG	$39.5244 - 0.19674i$	$40.5747 - 0.20105i$	$41.6408 - 0.20537i$	$42.7227 - 0.20972i$	$43.8204 - 0.21407i$
$\omega_{1,100}$	WKB	$39.7158 - 0.59020i$	$40.7712 - 0.60312i$	$41.8425 - 0.61610i$	$42.9297 - 0.62913i$	$44.0327 - 0.64220i$
	CNG	$39.5244 - 0.59021i$	$40.5747 - 0.60314i$	$41.6408 - 0.61612i$	$42.7227 - 0.62915i$	$43.8204 - 0.64222i$
$\omega_{2,100}$	WKB	$39.7137 - 0.98368i$	$40.7690 - 1.00523i$	$41.8403 - 1.02686i$	$42.9275 - 1.04857i$	$44.0304 - 1.07036i$
	CNG	$39.5244 - 0.98369i$	$40.5747 - 1.00523i$	$41.6408 - 1.02686i$	$42.7227 - 1.04858i$	$43.8204 - 1.07036i$
$\omega_{3,100}$	WKB	$39.7104 - 1.37721i$	$40.7658 - 1.40737i$	$41.8370 - 1.43765i$	$42.9241 - 1.46805i$	$44.0270 - 1.49855i$
	CNG	$39.5244 - 1.37716i$	$40.5747 - 1.40732i$	$41.6408 - 1.43761i$	$42.7227 - 1.46801i$	$43.8204 - 1.49851i$
$\omega_{4,100}$	WKB	$39.7061 - 1.77078i$	$40.7614 - 1.80955i$	$41.8326 - 1.84850i$	$42.9197 - 1.88758i$	$44.0225 - 1.92680i$
	CNG	$39.5244 - 1.77064i$	$40.5747 - 1.80941i$	$41.6408 - 1.84836i$	$42.7227 - 1.88744i$	$43.8204 - 1.92665i$

$$V(r) \simeq \frac{f(r)l^2}{r^2}, \tag{4.15}$$

where $f(r)$ is the g_{tt} component of the metric of the black hole. This means some high-order terms about $f(r)$ in the effective potential are ignored in the eikonal limit. For the self-dual black hole,

$$f(r) = 1 - \frac{2M}{r} + \frac{8(Mr - M^2)P}{r^2} - \frac{8(M^3 r - 5M^2 r^2 + 2Mr^3)P^2}{r^4} + \cdots, \tag{4.16}$$

where we have expanded Eq. (2.2) in the power of P and set a_0 equal to 0, because we only care the influence of P. One can find that Eq. (4.16) contains high-order terms of P. Then, in the eikonal limit, the effective potential (4.15) in this work indeed contains high-order terms of P. And, in fact, we have retained high-order terms of $f(r)$ in the effective potential when we use the WKB approximation method. So, our numerical results include the influence of higher order of the parameter P.

V. CONCLUSIONS AND DISCUSSIONS

In this work, we investigated the QNMs of the axial gravitational perturbation of the self-dual black hole with the fixed ADM mass in loop quantum gravity. Simulating the quantum correction by an effective anisotropic matter fluid, we obtained the master equation of the axial gravitational perturbation of the self-dual black hole. We considered the influence of the quantum parameter P, and found that the height of the effective potential increases with the parameter P. Using the WKB approximation method and the asymptotic iteration method, we calculated the QNMs of the axial gravitational perturbation of the self-dual black hole with different values of the parameter P. We

TABLE VI. The QNMs ω_{nl} of the axial gravitational perturbation of the self-dual black hole with different values of the parameter P and $l = 100$, calculated by the WKB approximation method and the QNMs-circular null geodesics (CNG) relation.

P		0	0.1	0.2	0.3	0.4
$\omega_{0,100}$	WKB	$38.6775 - 0.19244i$	$49.7817 - 0.23597i$	$62.3835 - 0.27936i$	$76.2699 - 0.31982i$	$91.0856 - 0.35422i$
	CNG	$38.4900 - 0.19245i$	$49.5404 - 0.23598i$	$62.0811 - 0.27937i$	$75.9001 - 0.31983i$	$90.6438 - 0.35423i$
$\omega_{1,100}$	WKB	$38.6764 - 0.57733i$	$49.7805 - 0.70792i$	$62.3823 - 0.83810i$	$76.2687 - 0.95946i$	$91.0845 - 1.06266i$
	CNG	$38.4900 - 0.57735i$	$49.5404 - 0.70794i$	$62.0811 - 0.83812i$	$75.9001 - 0.95948i$	$90.6438 - 1.06269i$
$\omega_{2,100}$	WKB	$38.6743 - 0.96225i$	$49.7781 - 1.17989i$	$62.3798 - 1.39686i$	$76.2663 - 1.59912i$	$91.0822 - 1.77113i$
	CNG	$38.4900 - 0.96225i$	$49.5404 - 1.17990i$	$62.0811 - 1.39687i$	$75.9001 - 1.59913i$	$90.6438 - 1.77114i$
$\omega_{3,100}$	WKB	$38.6711 - 1.34719i$	$49.7746 - 1.65191i$	$62.3762 - 1.95566i$	$76.2627 - 2.23882i$	$91.0788 - 2.47963i$
	CNG	$38.4900 - 1.34715i$	$49.5404 - 1.65186i$	$62.0811 - 1.95561i$	$75.9001 - 2.23878i$	$90.6438 - 2.47960i$
$\omega_{4,100}$	WKB	$38.6668 - 1.73219i$	$49.7699 - 2.12397i$	$62.3713 - 2.51451i$	$76.2578 - 2.87858i$	$91.0743 - 3.18818i$
	CNG	$38.4900 - 1.73205i$	$49.5404 - 2.12382i$	$62.0811 - 2.51436i$	$75.9001 - 2.87843i$	$90.6438 - 3.18806i$
P		0.5	0.6	0.7	0.8	0.9
$\omega_{0,100}$	WKB	$106.298 - 0.37938i$	$121.154 - 0.39247i$	$134.644 - 0.39203i$	$145.508 - 0.37995i$	$152.442 - 0.36427i$
	CNG	$105.782 - 0.37939i$	$120.566 - 0.39248i$	$133.990 - 0.39204i$	$144.801 - 0.37995i$	$151.702 - 0.36427i$
$\omega_{1,100}$	WKB	$106.297 - 1.13814i$	$121.153 - 1.17742i$	$134.643 - 1.17609i$	$145.507 - 1.13984i$	$152.441 - 1.09280i$
	CNG	$105.782 - 1.13816i$	$120.566 - 1.17744i$	$133.990 - 1.17611i$	$144.801 - 1.13986i$	$151.702 - 1.09282i$
$\omega_{2,100}$	WKB	$106.295 - 1.89692i$	$121.152 - 1.96238i$	$134.641 - 1.96015i$	$145.505 - 1.89974i$	$152.439 - 1.82134i$
	CNG	$105.782 - 1.89694i$	$120.566 - 1.96240i$	$133.990 - 1.96018i$	$144.801 - 1.89977i$	$151.702 - 1.82137i$
$\omega_{3,100}$	WKB	$106.292 - 2.65573i$	$121.149 - 2.74737i$	$134.639 - 2.74424i$	$145.502 - 2.65965i$	$152.436 - 2.54990i$
	CNG	$105.782 - 2.65572i$	$120.566 - 2.74736i$	$133.990 - 2.74425i$	$144.801 - 2.65967i$	$151.702 - 2.54992i$
$\omega_{4,100}$	WKB	$106.288 - 3.41459i$	$121.146 - 3.53239i$	$134.636 - 3.52835i$	$145.499 - 3.41958i$	$152.431 - 3.27847i$
	CNG	$105.782 - 3.41449i$	$120.566 - 3.53232i$	$133.990 - 3.52832i$	$144.801 - 3.41958i$	$151.702 - 3.27846i$

found that the parameter P has a positive effect on the absolute values of both the real part and imaginary part of the quasinormal frequency. This result is consistent with the conclusions for the QNMs of the perturbation of the scalar field and the electromagnetic field on the self-dual black hole with the fixed ADM mass [61,62]. In the eikonal limit, we obtained the relation between the QNMs and the parameters of the circular null geodesics in the self-dual black hole, and numerically verify it.

With more and more gravitational wave signals of compact binary components detected by the LIGO-Virgo-KAGRA collaboration and pictures of supermassive objects taken by the Event Horizon Telescope, it is possible to test gravitational theories in the strong gravitational field with multimessenger. And the coupling of electromagnetic and gravitational fields should be considered [69,70]. Cardoso *et al.* provided the parametrized black hole quasinormal ringdown in the general spherical symmetry background spacetime [71,72]. Völkel *et al.* got the bounds on modifications of black hole perturbation potentials near the light ring [73]. The shadow and ring of a black hole may exhibit rich behavior [74–78], and the relation between QNMs and shadow should be further explored. It would be interesting to find the constraints on the quantum correction parameters of the black holes in loop quantum gravity with the observed gravitational wave ringdown signals and pictures of black holes. And thermodynamics is also a fundamental property of black holes [79–81], the relation between QNMs and the thermodynamics of a black hole deserves attention. On the other hand, black holes always rotate in the real world, so the gravitational perturbations of the rotating black holes in loop quantum gravity and the related properties should be considered in future work.

ACKNOWLEDGMENTS

We thank Tao Zhu for important suggestion. This work was supported by National Key Research and Development Program of China (Grant No. 2020YFC2201503), the National Natural Science Foundation of China (Grants No. 12205129, No. 12147166, No. 11875151, No. 12075103, and No. 12247101), the China Postdoctoral Science Foundation (Grant No. 2021M701529), the 111 Project (Grant No. B20063), and Lanzhou City's scientific research funding subsidy to Lanzhou University.

[1] B. P. Abbott *et al.* (LIGO Scientific and Virgo Collaborations), Observation of Gravitational Waves from a Binary Black Hole Merger, Phys. Rev. Lett. **116**, 061102 (2016).

[2] R. G. Cai, Z. Cao, Z. K. Guo, S. J. Wang, and T. Yang, The gravitational-wave physics, Natl. Sci. Rev. **4**, 687 (2017).

[3] L. Bian, R. G. Cai, S. Cao, Z. Cao, H. Gao, Z. K. Guo, K. Lee, D. Li, J. Liu, Y. Lu *et al.*, The gravitational-wave physics II: Progress, Sci. China Phys. Mech. Astron. **64**, 120401 (2021).

[4] K. Akiyama *et al.* (Event Horizon Telescope Collaboration), First M87 event horizon telescope results. I. The shadow of the supermassive black hole, Astrophys. J. Lett. **875**, L1 (2019).

[5] K. Akiyama *et al.* (Event Horizon Telescope Collaboration), First M87 event horizon telescope results. II. Array and instrumentation, Astrophys. J. Lett. **875**, L2 (2019).

[6] K. Akiyama *et al.* (Event Horizon Telescope Collaboration), First M87 event horizon telescope results. III. Data processing and calibration, Astrophys. J. Lett. **875**, L3 (2019).

[7] K. Akiyama *et al.* (Event Horizon Telescope Collaboration), First M87 event horizon telescope results. IV. Imaging the central supermassive black hole, Astrophys. J. Lett. **875**, L4 (2019).

[8] K. Akiyama *et al.* (Event Horizon Telescope Collaboration), First M87 event horizon telescope results. V. Physical origin of the asymmetric ring, Astrophys. J. Lett. **875**, L5 (2019).

[9] K. Akiyama *et al.* (Event Horizon Telescope Collaboration), First M87 event horizon telescope results. VI. The shadow and mass of the central black hole, Astrophys. J. Lett. **875**, L6 (2019).

[10] K. Akiyama *et al.* (Event Horizon Telescope Collaboration), First Sagittarius A* event horizon telescope results. I. The shadow of the supermassive black hole in the center of the Milky Way, Astrophys. J. Lett. **930**, L12 (2022).

[11] K. Akiyama *et al.* (Event Horizon Telescope Collaboration), First Sagittarius A* event horizon telescope results. II. EHT and multiwavelength observations, data processing, and calibration, Astrophys. J. Lett. **930**, L13 (2022).

[12] K. Akiyama *et al.* (Event Horizon Telescope Collaboration), First Sagittarius A* event horizon telescope results. III. Imaging of the Galactic center supermassive black hole, Astrophys. J. Lett. **930**, L14 (2022).

[13] K. Akiyama *et al.* (Event Horizon Telescope Collaboration), First Sagittarius A* event horizon telescope results. IV. Variability, morphology, and black hole mass, Astrophys. J. Lett. **930**, L15 (2022).

[14] K. Akiyama *et al.* (Event Horizon Telescope Collaboration), First Sagittarius A* event horizon telescope results. V. Testing astrophysical models of the Galactic center black hole, Astrophys. J. Lett. **930**, L16 (2022).

[15] K. Akiyama *et al.* (Event Horizon Telescope Collaboration), First Sagittarius A* event horizon telescope results. VI. Testing the black hole metric, Astrophys. J. Lett. **930**, L17 (2022).

[16] B. P. Abbott *et al.* (LIGO Scientific and Virgo Collaborations), GWTC-1: A Gravitational-Wave Transient Catalog of Compact Binary Mergers Observed by LIGO and Virgo during the First and Second Observing Runs, Phys. Rev. X **9**, 031040 (2019).

[17] R. Abbott *et al.* (LIGO Scientific and Virgo Collaborations), GWTC-2: Compact Binary Coalescences Observed by LIGO and Virgo During the First Half of the Third Observing Run, Phys. Rev. X **11**, 021053 (2021).

[18] R. Abbott *et al.* (LIGO Scientific and Virgo Collaborations), GWTC-2.1: Deep extended catalog of compact binary coalescences observed by LIGO and Virgo during the first half of the third observing run, arXiv:2108.01045.

[19] R. Abbott *et al.* (LIGO Scientific, VIRGO, and KAGRA Collaborations), GWTC-3: Compact binary coalescences observed by LIGO and Virgo during the second part of the third observing run, arXiv:2111.03606.

[20] B. P. Abbott *et al.* (LIGO Scientific and Virgo Collaborations), Tests of General Relativity with GW150914, Phys. Rev. Lett. **116**, 221101 (2016); **121**, 129902(E) (2018).

[21] B. P. Abbott *et al.* (LIGO Scientific and Virgo Collaborations), Tests of general relativity with the binary black hole signals from the LIGO-Virgo catalog GWTC-1, Phys. Rev. D **100**, 104036 (2019).

[22] R. Abbott *et al.* (LIGO Scientific and Virgo Collaborations), Tests of general relativity with binary black holes from the second LIGO-Virgo gravitational-wave transient catalog, Phys. Rev. D **103**, 122002 (2021).

[23] R. Abbott *et al.* (LIGO Scientific, VIRGO, and KAGRA Collaborations), Tests of general relativity with GWTC-3, arXiv:2112.06861.

[24] S. Chandrasekhar, *The Mathematical Theory of Black Holes* (Oxford University Press, New York, 1983).

[25] M. Maggiore, *Gravitational Waves. Vol. 2: Astrophysics and Cosmology* (Oxford University Press, New York, 2018), ISBN: 978-0-19-857089-9.

[26] K. D. Kokkotas and B. G. Schmidt, Quasinormal modes of stars and black holes, Living Rev. Relativity **2**, 2 (1999).

[27] H. P. Nollert, TOPICAL REVIEW: Quasinormal modes: The characteristic 'sound' of black holes and neutron stars, Classical Quantum Gravity **16**, R159 (1999).

[28] E. Berti, V. Cardoso, and A. O. Starinets, Quasinormal modes of black holes and black branes, Classical Quantum Gravity **26**, 163001 (2009).

[29] R. A. Konoplya and A. Zhidenko, Quasinormal modes of black holes: From astrophysics to string theory, Rev. Mod. Phys. **83**, 793 (2011).

[30] S. Weinberg, *Gravitation and Cosmology: Principles and Applications of the General Theory of Relativity* (John Wiley and Sons, New York, 1972), ISBN 978-0-471-92567-5, 978-0-471-92567-5.

[31] T. Regge and J. A. Wheeler, Stability of a Schwarzschild singularity, Phys. Rev. **108**, 1063 (1957).

[32] F. J. Zerilli, Effective Potential for Even Parity Regge-Wheeler Gravitational Perturbation Equations, Phys. Rev. Lett. **24**, 737 (1970).

[33] V. Moncrief, Odd-parity stability of a Reissner-Nordstrom black hole, Phys. Rev. D **9**, 2707 (1974).

[34] V. Moncrief, Stability of Reissner-Nordstrom black holes, Phys. Rev. D **10**, 1057 (1974).

[35] S. A. Teukolsky, Rotating Black Holes—Separable Wave Equations for Gravitational and Electromagnetic Perturbations, Phys. Rev. Lett. **29**, 1114 (1972).

[36] B. Mashhoon, in *Proceedings of the Third Marcel Grossmann Meeting on Recent Developments of General*

Relativity, edited by H. Ning (North-Holland, Amsterdam, 1983), p. 599.
[37] B. F. Schutz and C. M. Will, Black hole normal modes: A semianalytic approach, Astrophys. J. Lett. **291**, L33 (1985).
[38] S. Iyer and C. M. Will, Black hole normal modes: A WKB approach. 1. Foundations and application of a higher order WKB analysis of potential barrier scattering, Phys. Rev. D **35**, 3621 (1987).
[39] R. A. Konoplya, Quasinormal behavior of the d-dimensional Schwarzschild black hole and higher order WKB approach, Phys. Rev. D **68**, 024018 (2003).
[40] J. Matyjasek and M. Opala, Quasinormal modes of black holes. The improved semianalytic approach, Phys. Rev. D **96**, 024011 (2017).
[41] R. A. Konoplya, A. Zhidenko, and A. F. Zinhailo, Higher order WKB formula for quasinormal modes and grey-body factors: Recipes for quick and accurate calculations, Classical Quantum Gravity **36**, 155002 (2019).
[42] H. T. Cho, A. S. Cornell, J. Doukas, T. R. Huang, and W. Naylor, A new approach to black hole quasinormal modes: A review of the asymptotic iteration method, Adv. Theor. Math. Phys. **2012**, 281705 (2012).
[43] L. Motl and A. Neitzke, Asymptotic black hole quasinormal frequencies, Adv. Theor. Math. Phys. **7**, 307 (2003).
[44] G. T. Horowitz and V. E. Hubeny, Quasinormal modes of AdS black holes and the approach to thermal equilibrium, Phys. Rev. D **62**, 024027 (2000).
[45] E. Berti, V. Cardoso, and P. Pani, Breit-Wigner resonances and the quasinormal modes of anti-de Sitter black holes, Phys. Rev. D **79**, 101501 (2009).
[46] E. W. Leaver, An analytic representation for the quasi normal modes of Kerr black holes, Proc. R. Soc. A **402**, 285 (1985).
[47] C. Rovelli, *Quantum Gravity* (Cambridge University Press, Cambridge, England, 2004), 10.1017/CBO9780511755804.
[48] L. Modesto and I. Premont-Schwarz, Self-dual black holes in LQG: Theory and phenomenology, Phys. Rev. D **80**, 064041 (2009).
[49] L. Modesto, Semiclassical loop quantum black hole, Int. J. Theor. Phys. **49**, 1649 (2010).
[50] E. Alesci and L. Modesto, Particle creation by loop black holes, Gen. Relativ. Gravit. **46**, 1656 (2014).
[51] A. Dasgupta, Entropy production and semiclassical gravity, SIGMA **9**, 013 (2013).
[52] A. Barrau, C. Rovelli, and F. Vidotto, Fast radio bursts and white hole signals, Phys. Rev. D **90**, 127503 (2014).
[53] S. Hossenfelder, L. Modesto, and I. Premont-Schwarz, Emission spectra of self-dual black holes, arXiv:1202.0412.
[54] S. Sahu, K. Lochan, and D. Narasimha, Gravitational lensing by self-dual black holes in loop quantum gravity, Phys. Rev. D **91**, 063001 (2015).
[55] T. Zhu and A. Wang, Observational tests of the self-dual spacetime in loop quantum gravity, Phys. Rev. D **102**, 124042 (2020).
[56] J. M. Yan, Q. Wu, C. Liu, T. Zhu, and A. Wang, Constraints on self-dual black hole in loop quantum gravity with S0-2 star in the Galactic center, J. Cosmol. Astropart. Phys. 09 (2022) 008.
[57] J. H. Chen and Y. J. Wang, Complex frequencies of a massless scalar field in loop quantum black hole spacetime, Chin. Phys. B **20**, 030401 (2011).
[58] J. S. Santos, M. B. Cruz, and F. A. Brito, Quasinormal modes of a massive scalar field nonminimally coupled to gravity in the spacetime of self-dual black hole, Eur. Phys. J. C **81**, 1082 (2021).
[59] M. B. Cruz, C. A. S. Silva, and F. A. Brito, Gravitational axial perturbations and quasinormal modes of loop quantum black holes, Eur. Phys. J. C **79**, 157 (2019).
[60] M. B. Cruz, F. A. Brito, and C. A. S. Silva, Polar gravitational perturbations and quasinormal modes of a loop quantum gravity black hole, Phys. Rev. D **102**, 044063 (2020).
[61] C. Liu, T. Zhu, Q. Wu, K. Jusufi, M. Jamil, M. Azreg-Aïnou, and A. Wang, Shadow and quasinormal modes of a rotating loop quantum black hole, Phys. Rev. D **101**, 084001 (2020); **103**, 089902(E) (2021).
[62] M. Momennia, Quasinormal modes of self-dual black holes in loop quantum gravity, Phys. Rev. D **106**, 024052 (2022).
[63] C. Y. Chen and P. Chen, Gravitational perturbations of nonsingular black holes in conformal gravity, Phys. Rev. D **99**, 104003 (2019).
[64] M. Bouhmadi-López, S. Brahma, C. Y. Chen, P. Chen, and D. h. Yeom, A consistent model of non-singular Schwarzschild black hole in loop quantum gravity and its quasinormal modes, J. Cosmol. Astropart. Phys. 07 (2020) 066.
[65] V. Cardoso, A. S. Miranda, E. Berti, H. Witek, and V. T. Zanchin, Geodesic stability, Lyapunov exponents and quasinormal modes, Phys. Rev. D **79**, 064016 (2009).
[66] V. Cardoso, J. P. S. Lemos, and S. Yoshida, Quasinormal modes of Schwarzschild black holes in four-dimensions and higher dimensions, Phys. Rev. D **69**, 044004 (2004).
[67] C. Gundlach, R. H. Price, and J. Pullin, Late time behavior of stellar collapse and explosions: 1. Linearized perturbations, Phys. Rev. D **49**, 883 (1994).
[68] R. A. Konoplya and Z. Stuchlík, Are eikonal quasinormal modes linked to the unstable circular null geodesics?, Phys. Lett. B **771**, 597 (2017).
[69] Y. Zou, M. Wang, and J. Jing, Test of a model coupling of electromagnetic and gravitational fields by using high-frequency gravitational waves, Sci. China Phys. Mech. Astron. **64**, 250411 (2021).
[70] W. D. Guo, Q. Tan, and Y. X. Liu, Gravito-electromagnetic coupled perturbations and quasinormal modes of a charged black hole with scalar hair, arXiv:2212.08784.
[71] V. Cardoso, M. Kimura, A. Maselli, E. Berti, C. F. B. Macedo, and R. McManus, Parametrized black hole quasinormal ringdown: Decoupled equations for nonrotating black holes, Phys. Rev. D **99**, 104077 (2019).
[72] R. McManus, E. Berti, C. F. B. Macedo, M. Kimura, A. Maselli, and V. Cardoso, Parametrized black hole quasinormal ringdown. II. Coupled equations and quadratic corrections for nonrotating black holes, Phys. Rev. D **100**, 044061 (2019).
[73] S. H. Völkel, N. Franchini, E. Barausse, and E. Berti, Constraining modifications of black hole perturbation potentials near the light ring with quasinormal modes, Phys. Rev. D **106**, 124036 (2022).

[74] W. B. Feng, S. J. Yang, Q. Tan, J. Yang, and Y. X. Liu, Overcharging a Reissner-Nordström Taub-NUT regular black hole, Sci. China Phys. Mech. Astron. **64**, 260411 (2021).
[75] Y. F. Cai, Remarkable effects of multiple photon spheres on black hole observations, Sci. China Phys. Mech. Astron. **65**, 120431 (2022).
[76] X. X. Zeng, K. J. He, and G. P. Li, Effects of dark matter on shadows and rings of Brane-World black holes illuminated by various accretions, Sci. China Phys. Mech. Astron. **65**, 290411 (2022).
[77] Y. Chen, G. Guo, P. Wang, H. Wu, and H. Yang, Appearance of an infalling star in black holes with multiple photon spheres, Sci. China Phys. Mech. Astron. **65**, 120412 (2022).
[78] X. Liu, S. Chen, and J. Jing, Polarization distribution in the image of a synchrotron emitting ring around a regular black hole, Sci. China Phys. Mech. Astron. **65**, 120411 (2022).
[79] S. W. Wei, Y. Q. Wang, Y. X. Liu, and R. B. Mann, Observing dynamic oscillatory behavior of triple points among black hole thermodynamic phase transitions, Sci. China Phys. Mech. Astron. **64**, 270411 (2021).
[80] R. G. Cai, Oscillatory behaviors near a black hole triple point, Sci. China Phys. Mech. Astron. **64**, 290432 (2021).
[81] S. Song, H. Li, Y. Ma, and C. Zhang, Entropy of black holes with arbitrary shapes in loop quantum gravity, Sci. China Phys. Mech. Astron. **64**, 120411 (2021).